43rd AIAA Aerospace Sciences Meeting and Exhibit
10 - 13 January 2005, Reno, Nevada

AIAA 2005-498

Comparison of Hybrid RANS/LES Turbulence Models on a Circular Cylinder at High Reynolds Number

R. H. Nichols*
The University of Alabama at Birmingham, Birmingham, AL 35294

Three hybrid RANS/LES turbulence models are applied to the flow over a three dimensional circular cylinder at high Reynolds number. Time-step and grid sensitivity studies are performed. The time-step study indicates that 200 steps per primary shedding cycle are required for temporal accuracy using a second order time implicit algorithm. The grid study indicates that some degree of grid independence can be achieved for the simulation of unsteady turbulent flows using these new turbulence models. As the mesh resolution is increased smaller scale turbulent structures become visible. A computational mesh with a grid resolution resulting in a ratio of the turbulent length scale to grid length scale greater than two produced a reasonable simulation with all three hybrid models.

Nomenclature

Cd	=	Drag coefficient
C_{DES}	=	Coefficient for SA-DES hybrid turbulence model
C_{DESKE}, C_{DESKW}	=	Coefficients for SST-DES hybrid turbulence model
Cl	=	Lift coefficient
d	=	Distance from the wall
$\tilde{d}$	=	Modified distance defined in Eq. (1)
F_1	=	SST model switching function
f_d	=	SST-MS hybrid model damping function defined in Eq. (8)
k	=	Turbulent kinetic energy
k_{LES}	=	Subgrid turbulent kinetic energy
k_{RANS}	=	RANS model turbulent kinetic energy
L_g	=	Local grid length scale
L_t	=	Local turbulent length scale
St	=	Strouhal Number
Δx, Δy, Δz	=	Local grid distance increments
β^*	=	SST model coefficient (0.09)
ε	=	Turbulent dissipation
ε_{RANS}	=	RANS turbulent dissipation
Λ	=	SST-MS model parameter defined in Eq. (9)
ν_t	=	Eddy viscosity
ν_{tLES}	=	Subgrid eddy viscosity
ν_{tRANS}	=	RANS eddy viscosity
Ω	=	Vorticity magnitude
ω	=	Specific dissipation

Introduction

SEVERAL investigators[1,2,3] have noted a limitation with traditional Reynolds Averaged Navier-Stokes (RANS) turbulence models when applied to unsteady flows. The RANS turbulence models produce too much eddy viscosity and over-damp the unsteady motion of the fluid. The problem is inherent in the construction of the RANS

* Research Associate Professor, Department of Mechanical Engineering. Senior Member AIAA.

turbulence models because of the assumption that all scales of the unsteady motion of the fluid are to be captured and modeled by the turbulence model. Spatially filtered turbulence models such as Large Eddy Simulation (LES) can provide improved results for simulating unsteady flows. LES models are currently limited to fairly low Reynolds numbers because of the grid sizes required to resolve the small-scale turbulent structures.

One approach to overcoming the shortcomings of RANS and LES models applied to unsteady flows at high Reynolds numbers is to spatially filter the RANS turbulence models such that the eddy viscosity does not include the energy of grid resolved turbulent scales. The spatially filtered RANS turbulence model may be thought of as an LES like subgrid model for very large turbulent eddies. This class of turbulence models has been called hybrid RANS/LES models because they incorporate aspects of both forms of turbulence modeling. These hybrid models maintain their RANS nature in the boundary layer region and transition to spatially filtered LES like models away from the body if the grid resolution is sufficiently fine in the region of interest. The hybrid models would be applicable to unsteady flows that are dominated by large-scale turbulent structure outside of the boundary layer. It is desirable that the spatial filter functions chosen not degrade the performance of the turbulence model when the largest turbulent scales present are below the resolution of the grid as is often the case in current aircraft CFD applications. Hybrid RANS/LES turbulence models have successfully been applied to several flows with large scale turbulent structure occurring outside the boundary layer.

This new class of turbulence models is inherently grid size dependent since increasing the grid resolution allows smaller and smaller turbulent scales to be resolved. This is both a strength and a weakness of this approach to turbulent flow simulation. It requires that the user be aware of the relevant turbulent scales when developing grid systems and choosing time steps to allow these scales to be simulated.

Several investigators have looked at the subsonic vortex cylinder shedding from a circular cylinder, but most of the work has been limited to lower Reynolds numbers than the present study. Travin, et. al[4] evaluated one hybrid RANS/LES model for Reynolds numbers ranging from $1.4\text{x}10^4$ to $3.0\text{x}10^6$ using a 5th order spatial upwind LES flow solver. Vatsa and Singer[5] applied the same hybrid RANS/LES model to cylinders with Reynolds numbers of $5\text{x}10^4$ to $1.5\text{x}10^5$ using a 2nd order spatial Navier-Stokes solver. Hansen and Forsythe[6] and Elmiligui, *et al.*[7] applied hybrid RANS/LES models to cylinders at a Reynolds number of $1.5\text{x}10^5$. Hansen and Forsythe included a grid refinement study. Turbulent boundary layer transition location is an issue at the lower Reynolds numbers of most of the studies. This work investigates grid and time step sensitivity for three hybrid RANS/LES turbulence models for the case of a circular cylinder at a Reynolds number of $8\text{x}10^6$ using a traditional 3rd order spatial upwind implicit solver.

Theory

There are two possibilities for developing hybrid models from existing RANS models. A first approach would be to modify the production or dissipation source terms in the turbulence model differential equations to include additional terms to adjust the local turbulence variables so that they do not include the grid realized contribution. This means that the turbulence quantities normally transported by the RANS turbulence model will be created or destroyed based on the local grid resolution.

A second approach would be to solve the existing RANS turbulence model in the normal manner and then filter the results to determine the level of eddy viscosity that will be used in the solution of the Navier-Stokes equations. This approach is somewhat simpler to develop since it requires no tuning of the differential transport equations and can be easily extended to different RANS turbulence models.

Spalart-Allmaras DES Model

Both approaches have been applied to unsteady flows. One example of the first form of a hybrid RANS/LES turbulence model based on the Spalart-Allmaras one-equation turbulence model[8] can be found in Ref. 3. The standard Spalart-Allmaras turbulence model contains a destruction term for eddy viscosity that is inversely proportional to the square of the distance from the wall (d). Spalart[3] suggests replacing the wall distance (d) in the destruction term with

$$\tilde{d} = \min\left(d, C_{DES} L_g\right) \tag{1}$$

where C_{DES} is a constant of O(1) and L_g is a grid length scale defined by

$$L_g = \max\left(\Delta x, \Delta y, \Delta z\right) \tag{2}$$

where Δx, Δy, and Δz are the local grid lengths. The modified destruction term has the effect of decreasing the eddy viscosity in regions of tight grid spacing. This modification causes the Spalart-Allmaras RANS turbulence model to behave like a Smagorinsky LES turbulence model when the grid spacing (L_g) is less than the distance from the wall, which is generally the case outside of the boundary layer. Note that the transition from RANS to LES does not include any turbulent length scale dependence, but is solely a function of the local grid spacing. Spalart[3] introduced the term Detached-Eddy Simulation (DES) to describe this model. DES has been applied to a number of unsteady flow problems including flow over a sphere[9], flow over a delta wing[10] and flow over an aircraft[11]. This model was used in the cylinder studies of Ref. 4, 5 and 6.

SST DES Model

Strelets[12] gives a similar modification to Menter's[13] Shear Stress Transport (SST) two-equation model. In this hybrid model the dissipation term (ε) in the turbulent kinetic energy equation (k) is replaced by

$$\varepsilon = \frac{\omega}{\beta^* k} = \frac{k^{3/2}}{\min\left(L_t, C_{DES} L_g\right)} = \frac{\varepsilon}{\min\left(1.0, C_{DES} \frac{L_g}{L_t}\right)} \tag{3}$$

where

$$L_t = \frac{\sqrt{k}}{\beta^* \omega} = \frac{k^{3/2}}{\varepsilon} \tag{4}$$

$$C_{DES} = (1 - F_1) C_{DESKE} + F_1 C_{DESKW} \tag{5}$$

Here ω is the specific dissipation, β^*=0.09, C_{DESKE}=0.61, and C_{DESKW}=0.78. The function F_1 is the SST turbulence model switching function. The turbulent dissipation ε defined in Eq. (3) is effectively increased when the grid size length scale L_g (Eq. (2)) is less than the turbulent length scale L_t (Eq. (4)). This causes the turbulent kinetic energy (k) and hence the eddy viscosity to be reduced in these regions. Unlike the one-equation Spalart-Allmaras DES model, this model does include a dependency on the local turbulent length scale. The turbulent length scale used in this model is a function of the filtered turbulent quantities. This model behaves like a k-equation LES subgrid model when the turbulent length scale is greater than the grid length scale, and the dissipation equation becomes decoupled from the kinetic energy equation in this region.

SST MS Model

Nichols and Nelson[14] give an example of the second approach for developing a hybrid RANS/LES turbulence model which they have designated a multi-scale model. The method was implemented in conjunction with the SST two-equation turbulence model. The SST model is solved using unfiltered turbulence quantities and the resulting eddy viscosity is filtered and passed to the Navier-Stokes solver. The *RANS* subscript denotes unfiltered quantities and the subscript *LES* is used to denote subgrid quantities. The turbulent length scale used in this effort is defined by

$$L_t = \max\left(6.0\sqrt{\nu_{tRANS} / \Omega}, k_{RANS}^{3/2} / \varepsilon_{RANS}\right) \tag{6}$$

where ν_{tRANS} is the unfiltered eddy viscosity and Ω is the local mean flow vorticity. This length scale is a mixture of the traditional turbulent scale definition for two-equation turbulence models ($k_{RANS}^{3/2} / \varepsilon_{RANS}$) and the definition usually associated with algebraic turbulence models ((ν_{tRANS}/Ω)$^{1/2}$). The turbulent length scale definition could be easily adapted to other types of turbulence models. The subgrid turbulent kinetic energy is defined as

$$k_{LES} = k_{RANS} f_d \tag{7}$$

The damping function is defined as

$$f_d = (1 + \tanh(2\pi(\Lambda - 0.5)))/2 \tag{8}$$

where

$$\Lambda = \frac{1.0}{1.0 + \left(\frac{L_t}{L_g}\right)^{4/3}} \tag{9}$$

and where L_g is defined in Eq. (2). The eddy viscosity is then calculated from

$$\nu_t = \nu_{tRANS} f_d + (1 - f_d)\nu_{tLES} \tag{10}$$

The LES based subgrid eddy viscosity is given by

$$\nu_{tLES} = \min(0.0854 L_g \sqrt{k_{LES}}, \nu_{\text{tRANS}}) \tag{11}$$

The multi-scale hybrid model behaves like a traditional SST model on the RANS end of the spectrum and transitions to a nonlinear *k*-equation model on the LES end of the spectrum. The switching function (f_d) in Eq. (10) was chosen to allow a smooth transition from the standard RANS turbulence model to the LES subgrid model. This hybrid RANS/LES approach can easily be extended to other RANS turbulence models with little to no alteration providing that a length scale can be derived for that model and a value for the turbulent kinetic energy can be approximated by that model. The multi-scale hybrid model, like the SST-DES model, transitions from RANS to LES as a function of the ratio of the local turbulent length scale predicted by the RANS model and the local grid spacing rather than being a function of the grid spacing alone as is the case for the Spalart-Allmaras DES model.

Nelson and Nichols[15] evaluated the Spalart-Allmaras DES and the SST multi-scale hybrid turbulence models as subgrid turbulence models for LES applications. The hybrid models were applied to a high-speed shear layer using a true LES flow solver. The study also included a number of traditional LES turbulence models. The results indicate that the hybrid models perform as well as more complicated LES subgrid models for the shear layer application.

Results

Unsteady three-dimensional calculations were performed for the vortex shedding from a circular cylinder for M=0.2 and Re_d=8x10^6. Three computational grids were used in the simulation:

Fine – 401x201x201
Mid – 201x101x101
Coarse – 101x51x51

The mid-level and coarse-level grids were constructed by removing every other point from the fine-level and mid-level grids respectively. The grids have a span of ten cylinder diameters. Periodic boundary conditions were applied at the side planes of the grid. The initial wall spacing was 2x10^{-4} diameters for the fine-level grid, which corresponds to a y+ of about 20. Wall function boundary[16] conditions were used in the calculations. All the calculations were performed using the NXAIR[17] overset structured implicit flow solver using 2nd order time, 3rd order upwind HHLEM[18] space, and 3 Newton subiterations per time step. An SSOR procedure was used to solve the unfactored solution matrix. The turbulence transport equations are solved time accurately loosely coupled with the mean flow equations within the Newton loop. The accuracy of NXAIR for unsteady flow applications is discussed in Ref. 19. The calculations were run 10,000 iterations and the final 4096 time steps were statistically analyzed. The centerline plane of the three grids is shown in Fig. 1.

Calculations with three different time steps were run on the mid-level grid with the multi-scale hybrid turbulence model to determine an acceptable time step for this simulation. The results are shown in Fig. 2. The primary shedding frequency for this example is just less than 60 Hz. These solutions correspond to 50, 200, and 800 time

steps per shedding cycle. The results from the largest time step are quite different from the smaller time step results. The spectral peak predicted with the large time step occurs at a much lower frequency than the peak predicted using the smaller time steps. Based on these results all subsequent simulations were performed using the 9.0E-5 second time step with 200 time steps per shedding cycle.

The data in Ref. 20 was obtained using both air (γ=1.4) and Freon (γ=1.13) as a test medium. Calculations were performed on the mid-level grid with the SST-MS hybrid model to assess the affect of test medium. The normal force spectral results are shown in Fig. 3. This indicates that the test medium is not an important factor at the conditions of this study. All subsequent solutions were performed using air as the test medium.

A comparison of the normal force power spectral density for the three hybrid models, the Spalart-Allmaras model, and the SST model for the mid-level grid are shown in Figure 4. The hybrid models show similar trends in that they all have a rather broad spectral peak at a Strouhal number of about 0.25. The two RANS models have a much narrower spectral peak at a similar Strouhal number. The RANS models have much lower energy away from the peak. This is an indication that the RANS models are providing too much damping of the unsteady solutions.

Instantaneous x-vorticity isosurfaces computed with the SST-DES hybrid turbulence model are shown in Fig. 5 for all three grids. The turbulent structure in the wake of the cylinder is clearly evident in the fine-level grid solution. The turbulent structure is reduced in the mid-level grid solution. There is very little structure present in the coarse-level grid solution.

Instantaneous contours of Mach number and eddy viscosity for the SA-DES, SST-DES, and SST-MS hybrid turbulence models computed on the three grid levels are shown in Fig. 6-11. All three hybrid turbulence models have similar trends on the three grid levels. Significant turbulent structure can be seen in the fine-level grid solutions with both large-scale and small-scale turbulent structure present. The mid-level solutions have large-scale structure present, but the smaller turbulent scales are absent. The mid-level grids also have structure that appears to be more periodic than does the fine-level grid solution. The coarse-level solutions show almost no turbulent structure and produce an almost steady state wake away from the cylinder. The level of eddy viscosity in the wake differs for the three turbulent models. The eddy viscosity for the SA-DES model shown in Fig. 7 indicates that this model effectively shuts off the eddy viscosity outside the boundary layer. The eddy viscosity for the SST-DES and the SST-MS models is reduced as the grid is refined. The SST-DES model tends to predict higher levels of eddy viscosity in the wake region than does the SST-MS model. The SST-DES model also predicts higher eddy viscosities along the edges of the wake than either the SA-DES or SST-MS models. Both the SST-DES and SST-MS models are tending toward a RANS type solution in the far wake of the coarse-level grid solution.

The ratio of the turbulent length scale to the local grid length scale for the SST-MS model is shown in Fig. 12 for the three grid levels. The length scale ratio seems to scale with the grid refinement for the mid-level to fine-level grid results, which indicates that the turbulent length scales predicted on the mid-level and fine-level grids are similar. The mid-level grid results in a length scale ratio of greater than two for most of the wake region. The coarse-level grid results indicate that the hybrid model is operating in the RANS mode.

The power spectral densities (PSD) of the axial normal force coefficient are shown in Figs. 13-15 for the three hybrid turbulence models. The mid-level and fine-level grid results are in general agreement to within the spectral resolution of the FFT for all three hybrid models. The coarse-level grid solutions are seen to be significantly different and the energy is contained in narrower peaks for all of the hybrid models. The coarse-level grid solutions are similar to the traditional RANS turbulence model results shown in Fig. 4 indicating that the hybrid models are operating in the RANS mode for most of the flow.

The average integrated drag coefficient (Cd) and the peak lift coefficient Strouhal number (St) for the three hybrid models computed on the three grid levels are shown along with experimental results[20,21,22] in Table 1. An estimate of the error due to the limited number of samples used in the computations of the average drag is also included in Table 1. This error was computed by conditionally sampling the CFD results and evaluating the variation of the average drag. The mid-level and fine-level grid results are in general agreement with the experimental data. These results are also in reasonable agreement with the results of Travin[4] obtained at a Reynolds number of 3.0×10^6. The coarse-level results for the hybrid models are in relative agreement with the RANS models on which they are based, indicating that the hybrid models are operating in RANS mode on this grid level. The hybrid models differ significantly from the RANS models on the mid-level grid. The error in the average drag is seen to increase with increasing grid refinement for all three models. This may be due to the additional turbulent scales that are present on the finer grids.

The percentage difference of the average drag and the Strouhal number relative to the fine grid solution is shown in Table 2. The grid refinement study did produce convergence in the predicted Strouhal number to within the frequency resolution of the FFT (ΔSt=0.013). The average drag for the SST-based hybrid models also reaches convergence within the sampling error shown in Table 1. The SA-DES hybrid model average drag does not reach

convergence on the grid levels tested here. The grid refinement study using the SA-DES model described in Ref. 6 also failed to produce grid convergence. The coarse-level grid is inadequate for all of the hybrid RANS/LES models tested.

Conclusion

These simulations indicate a fundamental difficulty in verification and validation for unsteady flows. As the grid is refined, smaller scale turbulent structures are resolved in the solution. This process will continue until the grid is refined below the Komologrov scale and all of the turbulent scales are grid resolved. The limiting grid refinement case cannot be approached with current computing hardware for most real world high Reynolds problems of interest. Comparison of statistical quantities derived from the unsteady solutions can be made to assure that the important features of the unsteady flow have been captured with a given grid, but the nature of the statistical analysis makes it difficult to assess whether a true "grid convergence" has been achieved.

The time step study indicated that about 200 time steps per primary shedding cycle were required for temporal accuracy with the SST-MS hybrid model. Using a larger time step causes the primary spectral peak to occur at a lower frequency than predicted with the smaller time step and than is seen in the data.

The simulations on the mid-level and fine-level grid systems using the SST-based hybrid models are in good general agreement indicating that a level of grid convergence can be achieved for the large turbulent scales with these models. The SA-DES model did not reach grid convergence for the average drag in this refinement study. The turbulent length scale to grid length scale ratio was greater than two in the wake region of the cylinder. This may serve as a rule of thumb for grid resolution for hybrid model applications. The coarse-level grid is inadequate for all of the hybrid RANS/LES models tested.

On the mid-level grid, the traditional RANS turbulence models tended to produce flows that display a single dominant shedding event as can be seen by the larger value of the normal force standard deviation. All of the hybrid turbulence models produce solutions with a much broader spectral peak than the peak produced by the RANS models on the mid-level and fine-level grids. This indicates that the hybrid models are allowing weaker turbulent structures at scales away from the primary shedding scale to exist. These weaker structures are being damped in the RANS solutions. Both the RANS and the hybrid models produce similar solutions on the coarse-level grid, indicating that the hybrid models are operating in the RANS mode for the most part.

The hybrid RANS/LES turbulence models are relatively new and will need to be exercised for a wide variety of problems to determine their accuracy before they become an accepted tool for fluid modelers. They seem to offer much for unsteady flow applications, but issues such as grid sensitivity need to be further addressed. Hopefully more effort will go into these models in the near future so that they can be matured for use in everyday applications.

Acknowledgments

This publication made possible through support provided by DoD High Performance Computing Modernization Program (HPCMP) Programming Environment and Training (PET) activities through Mississippi State University under terms of Contract No. N62306-01-D-7110.

References

[1]Nichols, R. and Tramel, R., "Applications of a Highly Efficient Numerical Method for Overset Mesh Moving Body Problems," AIAA-97-2255, June 1997.

[2]Sinha, N., Dash, S., and Chidambaram, N., "A Perspective on the Simulation of Cavity Aeroacoustics," AIAA-98-0286, Jan. 1998.

[3]Spalart, P., Jou, W.-H., Strelets, M., and Allmaras, S., "Comments on the Feasibility of LES for Wings and on a Hybrid RANS/LES Approach," Eds. C. Liu and Z. Liu, Greyden Press, Columbus, OH, August 1997.

[4]Travin, A., Shur, M., Strelets, M. and Spalart, P., "Detached-Eddy Simulations Past a Circular Cylinder," *Flow, Turbulence and Combustion*, Vol. 63, pp 293-313, 1999.

[5]Vatsa, V. N. and Singer, B. A., "Evaluation of a Second-Order Accurate Navier-Stokes Code for Detached Eddy Simulation Past a Circular Cylinder," AIAA-2003-4085, Jun. 2003.

[6]Hansen, R. P. and Forsythe, J. R., "Large and Detached Eddy Simulations of Flow over a Circular Cylinder using Unstructured Grids," AIAA-2003-0775, Jan. 2003.

[7]Elmiligui, A., Abdol-Hamid, K., Massey, S., and Pao, S., "Numerical Study of Flow Past a Circular Cylinder Using RANS, Hybrid RANS/LES and PANS Formulations," AIAA-2004-4959, Aug. 2004.

[8]Spalart, P. R. and Allmaras, S. R., "A One-Equation Turbulence Model for Aerodynamic Flows," AIAA-92-0439, Jan. 1992.

[9]Constatinescu, G. and Squires, K., "LES and DES Investigations of the Turbulent Flow over a Sphere," AIAA-2000-0540, Jan. 2000.

[10]Mitchell, A., Morton, S., and Forsythe, J., "Analysis of Delta Wing Vortical Substructures using Detached-Eddy Simulation," AIAA-2002-2968, Jun. 2002.
[11]Forsythe, J., Squires, K., Wurtzler, K., and Spalart, P, "Detached-Eddy Simulation of Fighter Aircraft at High Alpha," AIAA-2002-0591.
[12]Strelets, M., "Detached Eddy Simulation of Massively Separated Flows," AIAA-2001-0879, Jan. 2001.
[13]Menter, F. R. and Rumsey, C. L., "Assessment of Two-Equation Turbulence Models for Transonic Flows," AIAA-94-2343, June 1994.
[14]Nichols, R. and Nelson, C., "Applications of Hybrid RANS/LES Turbulence Models," AIAA-2003-0083, Jan. 2003.
[15]Nelson, C. and Nichols, R., "Evaluation of Hybrid RANS/LES Turbulence Models using an LES Code," AIAA-2003-3552, Jun. 2003.
[16]Tramel, R. W. and Nichols, R. H., "A Highly Efficient Numerical Method for Overset-Mesh Moving–Body Problems," AIAA-97-2040, June 1997.
[17]Einfeldt, B., Munz, C. D. Roe, P. L., and Sjogreen, B., "On Godunov-Type Methods Near Low Densities," *Journal of Computational Physics*, Vol. 92, No. 2, 1991, pp. 273-295.
[18]Nichols, R. H. and Nelson, C. C., "Wall Function Boundary Conditions Including Heat Transfer and Compressibility," *AIAA Journal*, Vol. 42, No. 6, pp 1107-1114, June 2004.
[19]Nichols, R. H. and Heikkinen, B. D., "Validation of Implicit Algorithms for Unsteady Flows Including Moving and Deforming Grids," AIAA-2005-0683, Jan. 2005.
[20]Jones, G.W., Cincotta, J.J., and Walker, R. W., "Aerodynamic Forces on a Stationary and Oscillating Circular Cylinder at High Reynolds Number," NASA-TR-R-300, October 1968.
[21]Roshko, A., "Experiments on the Flow Past a Circular Cylinder at Very High Reynolds Number," *Journal of Fluid Mechanics*, Vol. 10, Part 3, May 1961, pp. 345-356.
[22]Schlichting,H., *Boundary Layer Theory,* 7th Edition, McGraw-Hill, New York, 1979.

Model	Grid	Average Cd	CFD Cd Error (%)	St
SA	Coarse	0.27	5.5	0.220
SST	Coarse	0.19	0	0.232
SA-DES	Coarse	0.30	0.5	0.220
SST-DES	Coarse	0.22	0.2	0.232
SST-MS	Coarse	0.20	0	0.232
SA	Mid	0.51	0.1	0.269
SST	Mid	0.52	0	0.269
SA-DES	Mid	0.63	1.5	0.256
SST-DES	Mid	0.59	1.0	0.256
SST-MS	Mid	0.55	3.4	0.269
SA-DES	Fine	0.52	2.3	0.244
SST-DES	Fine	0.59	7.9	0.244
SST-MS	Fine	0.58	3.3	0.256
DATA[20]		0.51-0.54	-	0.31
DATA[21]		0.79	-	0.27
DATA[22]		-	-	0.29
SA-DES[4]		0.41-0.51	-	0.33-0.35

Table 1. Force coefficient and Strouhal number predictions on the 3D circular cylinder.

Model	Grid	Difference in Average Cd (%)	Difference in St (%)
SA-DES	Coarse	52.4%	9.8%
SST-DES	Coarse	62.7%	4.9%
SST-MS	Coarse	65.5%	9.4%
SA-DES	Mid	21.2%	4.9%
SST-DES	Mid	0%	4.9%
SST-MS	Mid	5.2%	5.1%

Table 2. Grid refinement study error relative to the fine grid.

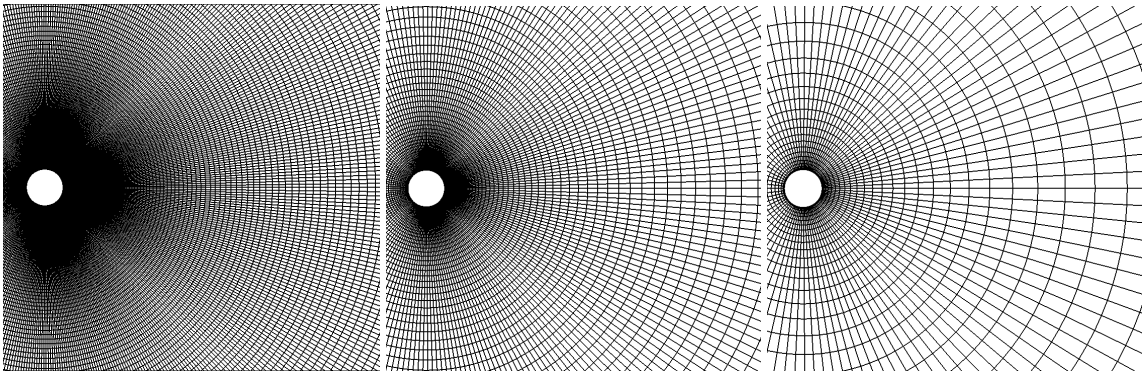

Fine Grid Mid Grid Coarse Grid

Figure 1. Cylinder grid centerline.

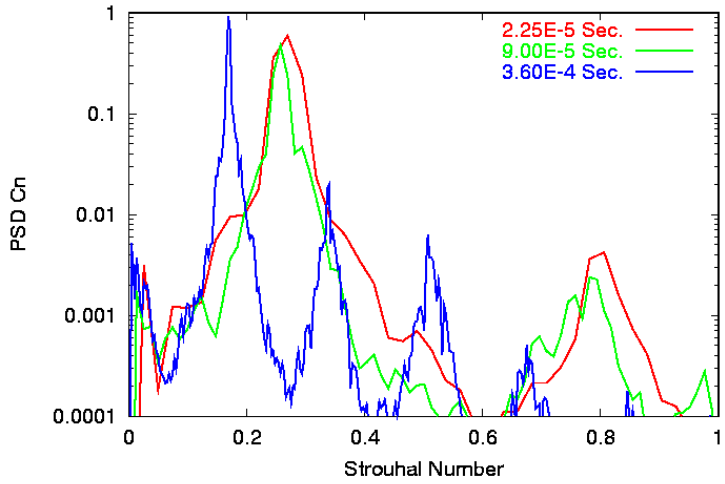

Figure 2. Normal force power spectral density for 3 different time steps.

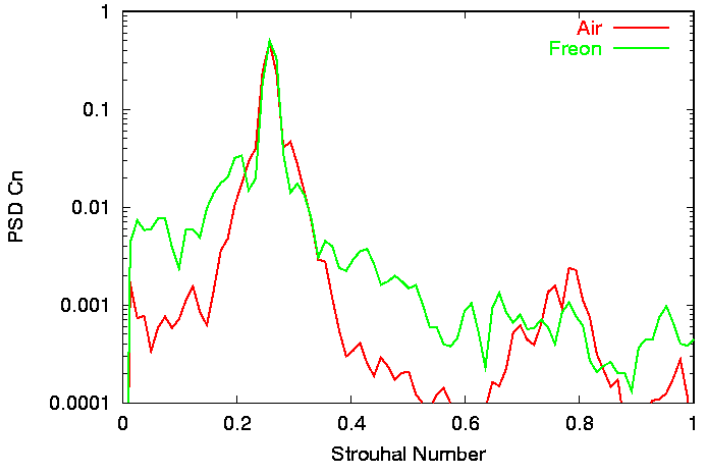

Figure 3. Normal force power spectral density for air and Freon using the SST-MS hybrid model.

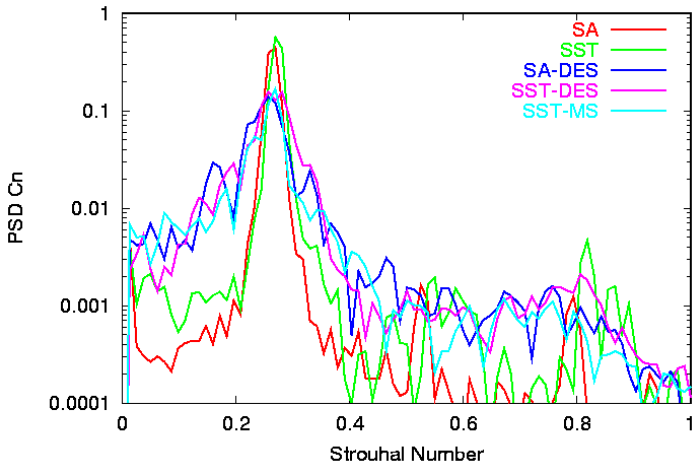

Figure 4. Normal force power spectral density on the mid-level grid.

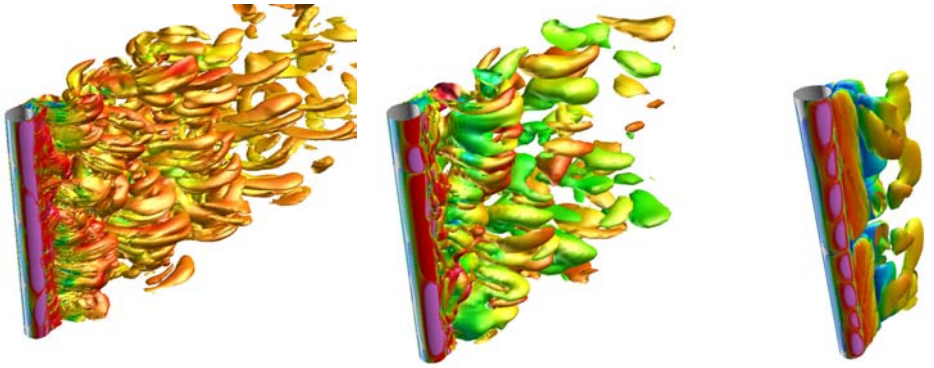

Fine Grid Mid Grid Coarse Grid

Figure 5. Instantaneous vorticity isosurfaces colored by Mach number for the SST-DES hybrid turbulence model.

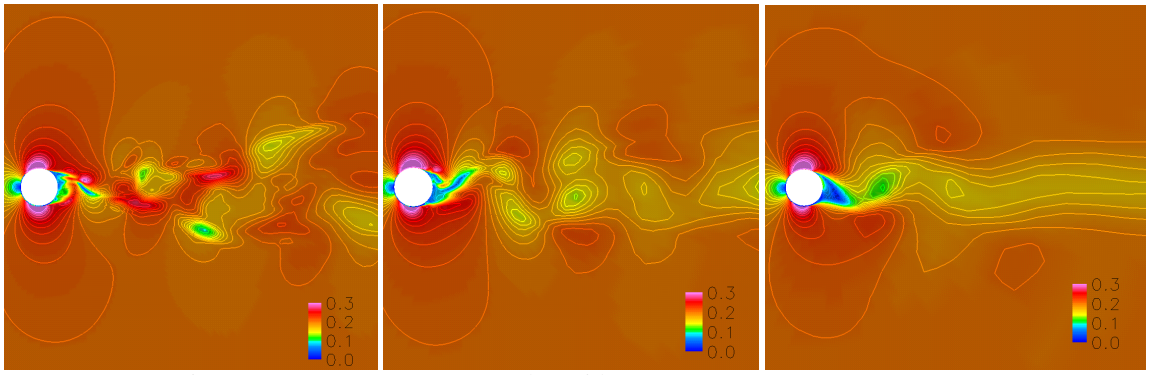

a. Fine b. Mid c. Coarse

Figure 6. Instantaneous Mach number contours for the SA-DES hybrid turbulence model.

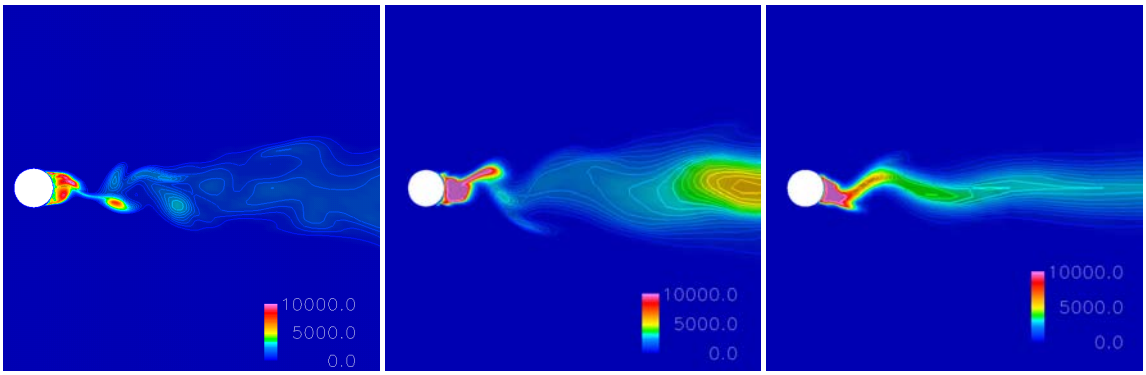

a. Fine b. Mid c. Coarse

Figure 7. Instantaneous eddy viscosity contours for the SA-DES hybrid turbulence model.

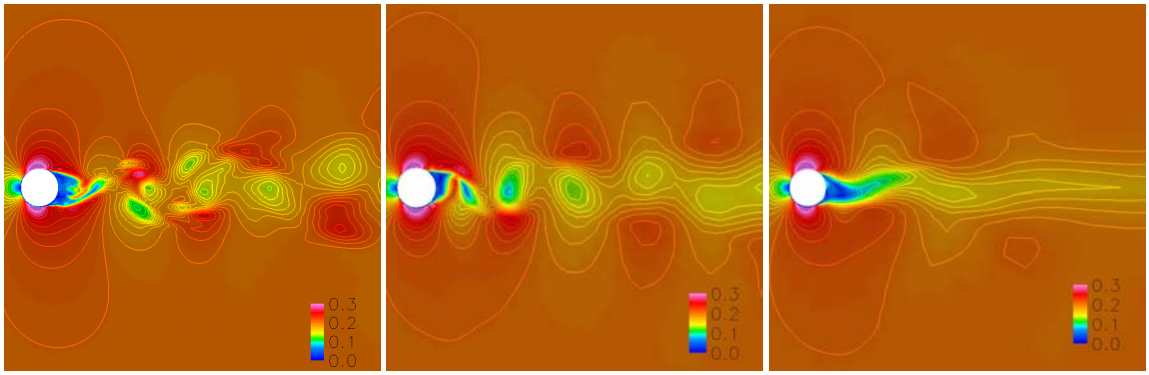

a. Fine b. Mid c. Coarse

Figure 8. Instantaneous Mach number contours for the SST-DES hybrid turbulence model.

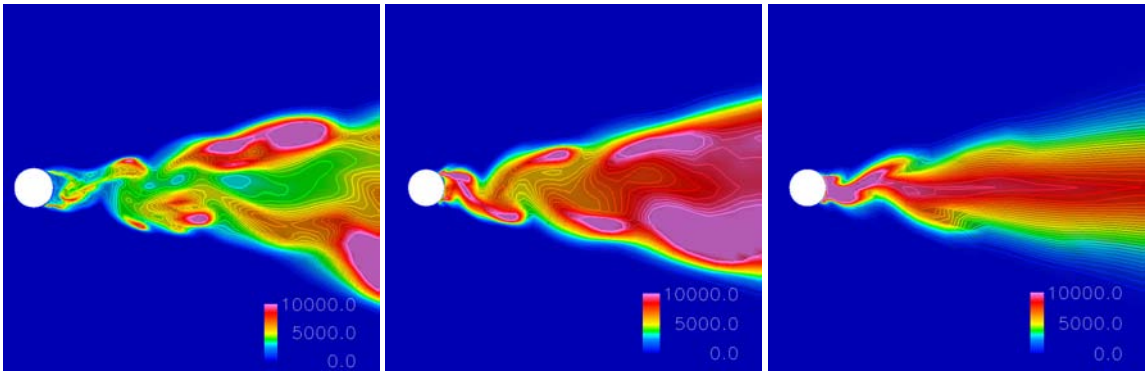

a. Fine b. Mid c. Coarse

Figure 9. Instantaneous eddy viscosity contours for the SST-DES hybrid turbulence model.

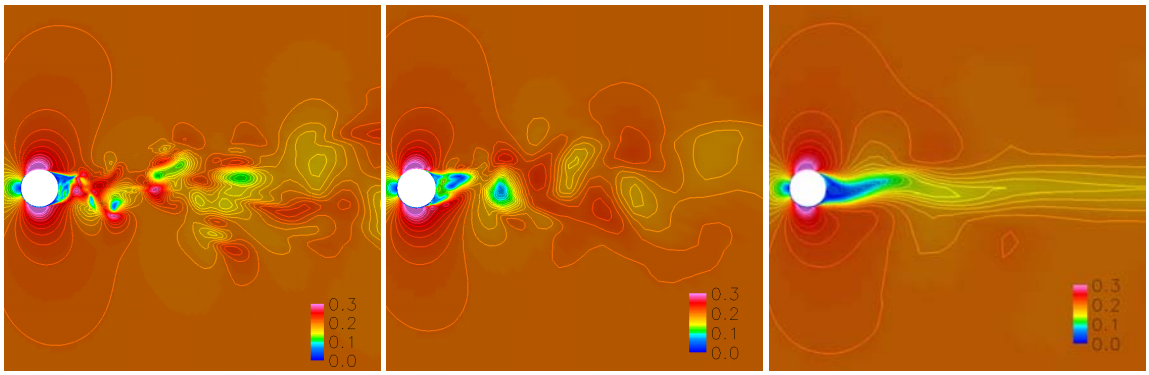

a. Fine b. Mid c. Coarse

Figure 10. Instantaneous Mach number contours for the SST-MS hybrid turbulence model.

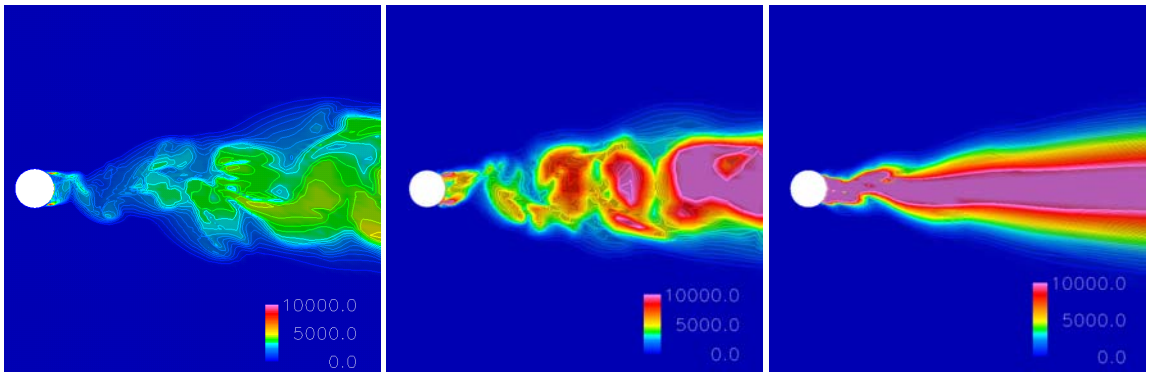

a. Fine b. Mid c. Coarse

Figure 11. Instantaneous eddy viscosity contours for the SST-MS hybrid turbulence model.

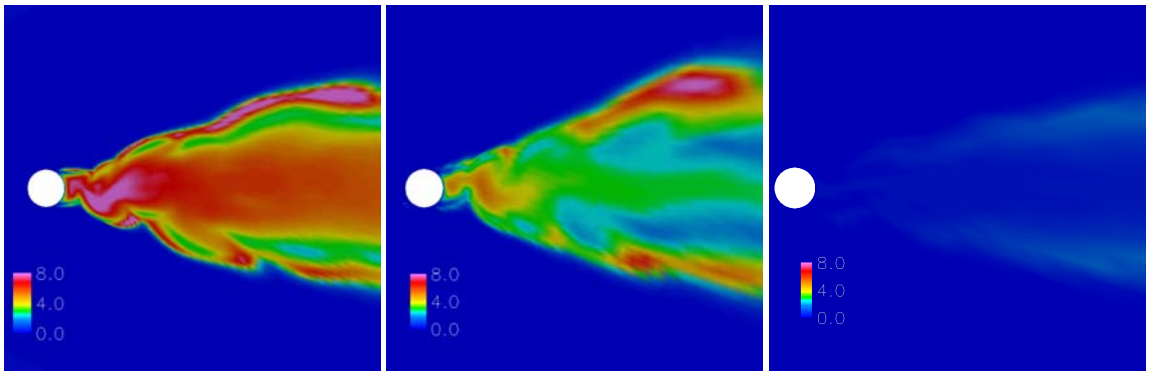

a. Fine b. Mid c. Coarse

Figure 12. Instantaneous ratio of turbulent length scale to the grid length scale for the SST-MS hybrid turbulence model.

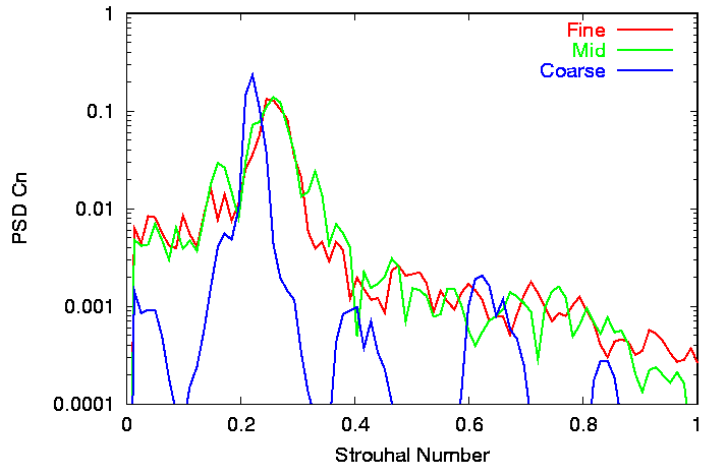

Figure 13. Power spectral density of the normal force coefficient for the SA-DES hybrid model.

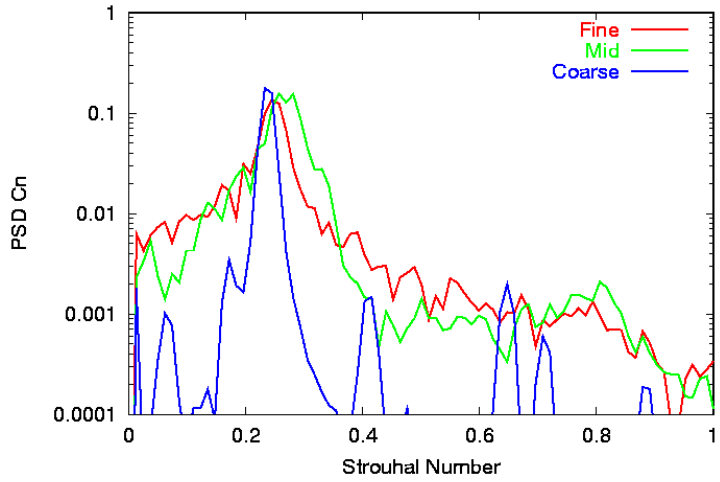

Figure 14. Power spectral density of the normal force coefficient for the SST-DES hybrid model.

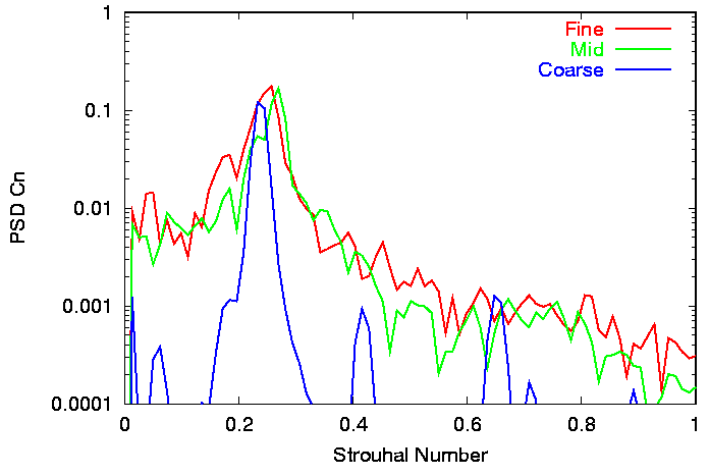

Figure 15. Power spectral density of the normal force coefficient for the SST-MS hybrid model.